JOURNAL OF ENVIRONMENTAL SCIENCES 135 (2024) 367–378

Available online at www.sciencedirect.com

ScienceDirect

www.elsevier.com/locate/jes

JES JOURNAL OF ENVIRONMENTAL SCIENCES

www.jesc.ac.cn

Research Article

Effects of operating conditions on iron (hydr)oxides evolution and ciprofloxacin degradation in potassium ferrate-ozone stepwise oxidation system

Xiaochen Li[1,**], *Yifan Wang*[1,**], *Ning Wang*[1], *Mei Li*[1], *Maomao Bai*[1], *Jingtao Xu*[1], *Hongbo Wang*[1,2,*]

[1] *School of Municipal and Environmental Engineering, Shandong Jianzhu University, Jinan 250101, China*
[2] *Resources and Environment Innovation Institute, Shandong Jianzhu University, Jinan 250101, China*

ARTICLE INFO

Article history:
Received 18 October 2022
Revised 13 December 2022
Accepted 13 December 2022
Available online 21 December 2022

Keywords:
Potassium ferrate reduction products
Catalytic ozonation
Ciprofloxacin
Potassium ferrate pre-oxidation time

ABSTRACT

In this study, a stepwise oxidation system of potassium ferrate (K_2FeO_4) combined with ozone (O_3) was used to degrade ciprofloxacin (CIP). The effects of pH and pre-oxidation time of K_2FeO_4 on the evolution of K_2FeO_4 reduction products (iron (hydr)oxides) and CIP degradation were investigated. It was found that in addition to its own oxidation capacity, K_2FeO_4 can also influence the treatment effect of CIP by changing the catalyst content. The presence of iron (hydr)oxides effectively enhanced the mineralization rate of CIP by catalyzing ozonation. The pH value can influence the content and types of the components with catalytic ozonation effect in iron (hydr)oxides. The K_2FeO_4 pre-oxidation stage can produce more iron (hydr)oxides with catalytic components for subsequent ozonation, but the evolution of iron (hydr)oxides components was influenced by O_3 treatment. It can also avoid the waste of oxidation capacity owing to the oxidation of iron (hydr)oxides by O_3 and free radicals. The intermediate degradation products were identified by Fourier transform ion cyclotron resonance mass spectrometry (FT-ICR-MS). Besides, the degradation pathways were proposed. Among the degradation products of CIP, the product with broken quinolone ring structure only appeared in the stepwise oxidation system.

* Corresponding author.
E-mail: wanghongbo@sdjzu.edu.cn (H. Wang).
** These authors contributed equally to this work.

https://doi.org/10.1016/j.jes.2022.12.018
1001-0742/

Introduction

Ciprofloxacin (CIP) is a kind of fluoroquinolone (FQ) antibiotics which has been widely used for respiratory infections in humans and animals (Porras et al., 2016). It is usually directly discharged into the municipal sewage system without targeted treatment. However, conventional sewage treatment technologies (activated sludge, adsorption, flocculation, etc.) can only partially transfer CIP into the sludge phase and cannot achieve thorough degradation and removal of it.

The degradation of CIP has been reported in a small amount of literature (Mahdi-Ahmed and Chiron, 2014; Porras et al., 2016; Zhang et al., 2015). Unfortunately, the structure of quinolone, an effective antibiotic site with pharmacological activity (preventing DNA unwinding and replication), was still integrated in their studies (Liu et al., 2013). As a result, the residues still had antibacterial activity (Zhang et al., 2015), which would cause microorganisms to develop resistance to antibiotics (Kim et al., 2020). Therefore, further degradation and removal of CIP residues in effluent from the sewage treatment plant, especially from the secondary effluent, is crucially important (Breazeal et al., 2013).

Ozonation is regarded as one of the most promising methods to deal with the discharge of trace pollutants from secondary effluent of sewage treatment plants (Zimmermann et al., 2012). Moreover, it was also reported for the treatment of quinolone antibiotics (De Witte et al., 2010; Iakovides et al., 2019; Ling et al., 2018). Ozonation is a mature technology that utilizes the high oxidation potential and strong reactivity of ozone (O_3). It can not only directly oxidize pollutants, but also indirectly oxidize them utilizing ·OH generated by O_3 decomposition (Li et al., 2020; Wang and Xu, 2012). However, the limited mass transfer efficiency of O_3 in water restricts its utilization efficiency (Chen and Wang, 2021). Besides, the selectivity of ozonation results in slow oxidation rate and low mineralization rate for some organic pollutants. Therefore, ozonation cannot completely degrade some refractory intermediates (such as carboxylic acids and aldehydes, etc.) (Wang and Chen, 2020). Currently, the catalytic ozonation technology using metal oxides (Li et al., 2018; Nemati Sani et al., 2019) as catalysts to stimulate O_3 to efficiently produce ·OH has been developed and become an effective treatment method for antibiotics degradation (Chen and Wang, 2019; Nemati Sani et al., 2019; Yuan et al., 2019). However, the generation of disinfection by-products (DBPs) is also a challenge as O_3 and ·OH can lead to the formation of bromate intermediates ($HOBr/OBr^-$) (Von Gunten, 1998).

Ferrate(VI) is a versatile green oxidant that can effectively avoid the formation of DBPs during ozonation process (Li et al., 2009; Zheng et al., 2021). Besides, it has been documented that the reduced potassium ferrate (K_2FeO_4) can form iron (hydr)oxides containing FeOOH and Fe_2O_3 (Prucek et al., 2013), which can play a catalytic role in ozonation (Wang and Bai, 2017). Therefore, K_2FeO_4 combined with O_3 may become an excellent choice to supplement the limitations of catalytic ozonation by metal oxide. Accordingly, a stepwise oxidation system of K_2FeO_4 combined with O_3 was constructed. At present, there are few studies on the combination of ferrate (VI) and O_3 (Han et al., 2019; Han et al., 2013; Liu et al., 2018). As far as we know, few of them have focused on the effect of operating conditions on the types and conversions of iron (hydr)oxides.

Therefore, the objectives of this study were: (1) to verify the feasibility of the stepwise oxidation system for CIP degradation and to investigate the effect of K_2FeO_4 dosage on the stepwise oxidation system from the perspective of iron (hydr)oxides, (2) to investigate the effect of pH on the formation of iron (hydr)oxides in the stepwise oxidation system, (3) to explore the effect of K_2FeO_4 pre-oxidation time on the formation of iron (hydr)oxides, (4) to propose the possible degradation pathways of CIP in the step oxidation system.

1. Materials and methods

1.1. Experimental setup and reagents

Ciprofloxacin (CIP, $C_{17}H_{18}FN_3O_3$, purity ≥ 98%, CAS No.: 85721-33-1) was purchased from Aladdin Reagent (Shanghai) Co., Ltd, China. Sodium thiosulphate ($Na_2S_2O_3·5H_2O$), boric acid (H_3BO_3), borax ($Na_2B_4O_7·10H_2O$), phosphoric acid (H_3PO_4), sodium hydroxide (NaOH), and hydrochloric acid (HCl) were obtained from Sinopharm Chemical Reagent Co., Ltd. All the above chemicals are of analytical grade. Acetonitrile, formic acid (purity ≥ 98%), triethylamine, and methanol used for chromatographic analysis were obtained from Tianjin Kemiou Chemical Reagent Co., Ltd., all of which were of HPLC grade. Solid K_2FeO_4 (purity ≥ 90%) was prepared by electrolysis in our laboratory, stored in a brown glass bottle, and placed in a desiccator. The purity of K_2FeO_4 was determined by UV spectrophotometry before each use.

The reactor was designed and installed as shown in Appendix A **Fig. S1**, which was similar as described in our previous study (Wang et al., 2022).

1.2. Process design and operation

As shown in Appendix A **Fig. S1**, the experiments were carried out in a 5 L K_2FeO_4 reactor and an 1 L O_3 reactor (the dimensions of the glass reactor were 40 mm × 850 mm (diameter × height, respectively)). The details of batch experiments are provided in Appendix A. Briefly, the CIP with a concentration of 20 μmol/L was firstly pre-oxidized by feeding the solid K_2FeO_4 from the top of the K_2FeO_4 reactor, and stirred at 70 r/min during this process. After a certain period, the peristaltic pump was used to carry the pre-oxidized water sample into the O_3 reactor for catalytic ozonation. The samples were taken out of the sample tap at certain time intervals, and 0.1 mol/L sodium thiosulfate was added dropwise to remove residual O_3 to terminate the reaction. All samples were filtered through 0.45 μm cellulose acetate filters to remove insoluble impurities and other particles before analysis. The O_3 was generated by an O_3 generator (Model ETX 120, Tonglin, China). An O_3 detector (Model 3S-J5000, Tonglin, China) was used to measure the concentrations of O_3 gas. The presence or absence of K_2FeO_4 reduction products during the process was distinguished and controlled with 0.45 μm cellulose acetate filters.

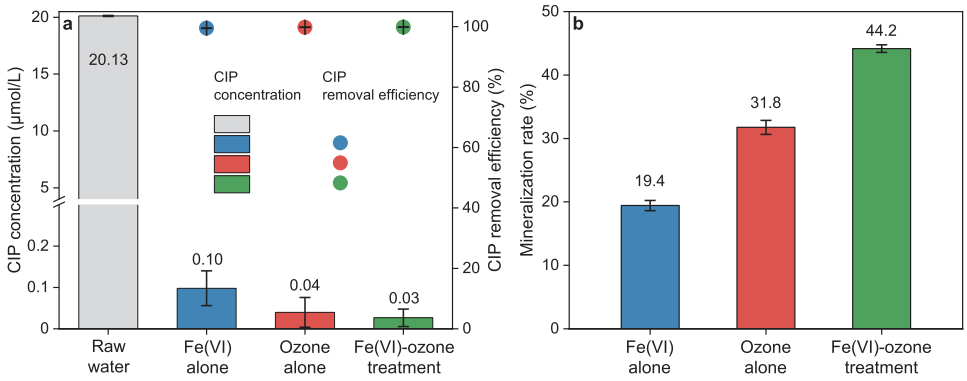

Fig. 1 – Variation of (a) concentrations and (b) mineralization rates of CIP by different treatments (CIP = 20 μmol/L, K_2FeO_4 = 450 μmol/L, O_3 = 17 mg/L, pH 7 buffer system, *t* = 15 min).

1.3. *Analytical method*

The CIP concentration in water was determined using high performance liquid chromatography (HPLC, waters 2996, USA) equipped with a reversed-phase C18 column (250 mm × 4.6 mm, 5 μm) and a UV detector. The mobile phase was a mixed solution of acetonitrile and 0.025 mol/L phosphoric acid solution (adjusted to pH = 3.0 ± 0.1 with triethylamine) with a ratio of 17:83 (V/V). The detection wavelength was 278 nm.

The intermediate products formed after the stepwise oxidation of CIP were identified and speculated by Fourier transform ion cyclotron resonance mass spectrometry (FT-ICR-MS, Waters, USA). The details are provided in Appendix A.

Fourier transform infrared spectrometer (ENSOR, Brooke, Germany) was used to identify the functional group composition of iron (hydr)oxides. Total organic carbon (TOC) was determined by a TOC analyzer (TOC-VCPH, Shimadzu Corporation, Japan). The pH value changes were monitored by a multiparameter water quality detector (Multi3620 IDS, Xylem, Germany).

2. Results and discussion

2.1. *Degradation and mineralization of CIP*

The degradation and mineralization of CIP by different treatments are shown in Fig. 1. As can be seen from Fig. 1a, 20 μmol/L CIP can be effectively degraded by all three treatment methods after 15 min, and the removal efficiencies were above 99%. The stepwise oxidation system of K_2FeO_4 combined with O_3 had no significant advantage over the single oxidation system. However, in terms of the mineralization rate of CIP, there were significant differences among different treatments (Fig. 1b). Although either O_3 treatment alone or K_2FeO_4 treatment alone can effectively degrade CIP, the mineralization rate after each individual treatment was only about 31.8% and 19.4%, respectively. In contrast, the mineralization rate increased significantly to 44.2% after the stepwise oxidation treatment. This phenomenon indicated that O_3 or K_2FeO_4 can react easily with CIP and reduce it to a low concentration in water, but the oxidation capacity of single oxidation treatment can only achieve a low CIP mineralization rate. The high removal efficiency of CIP was mainly due to the conversion of the broken piperazine ring into a variety of intermediate products. Single oxidation treatment was difficult to further degrade the converted intermediate products. For comparison, the ·OH generated by the direct decomposition of K_2FeO_4 and O_3 can be used in the stepwise oxidation process (Fe(VI) → Fe(V) → Fe(III) + H_2O_2, Fe(VI) → Fe(IV) → Fe(II), Fe(II) + H_2O_2 → ·OH + Fe(III) (Lee et al., 2014; Sharma et al., 2015), $O_3 + OH^- \rightarrow O_2^- + HO_2\cdot \rightarrow \cdot OH$). On the other hand, the iron (hydr)oxides produced by the reduction of K_2FeO_4 are rich in surface hydroxyl groups (Prucek et al., 2013; Prucek et al., 2015), which can catalyze O_3 decomposition and promote the generation of ·OH. It can produce more ·OH than single oxidation treatment (Liu et al., 2018), and therefore further enhance the mineralization rate.

2.1.1. *The role of K_2FeO_4 in the stepwise oxidation treatment of CIP*

Fig. 2 clearly demonstrates that the CIP removal efficiency reached more than 94% in the K_2FeO_4 (50 μmol/L) treatment stage of the stepwise oxidation process, and further reached over 99% after catalytic ozonation stage. With the increase in K_2FeO_4 dosage, the removal efficiency of CIP increased from 94.8% (50 μmol/L K_2FeO_4) to 99.5% (450 μmol/L K_2FeO_4) in the K_2FeO_4 treatment stage. Even at a dosage of 50 μmol/L K_2FeO_4, the CIP removal efficiency can reach more than 99% after the stepwise oxidation treatment. The complete removal of the CIP precursors was achieved at the dosage of 50–450 μmol/L K_2FeO_4.

To verify that K_2FeO_4 did not only play a pre-oxidation role in the process of stepwise oxidation of CIP, the water samples after K_2FeO_4 treatment were treated differently. One group was directly treated with O_3. The other group was firstly filtered to remove iron (hydr)oxides, and then treated with O_3. Experiments were carried out under four dosage conditions of K_2FeO_4.

As shown in Fig. 3, during the K_2FeO_4 treatment stage, when the K_2FeO_4 dosage was 50, 150, 300, and 450 μmol/L, the CIP mineralization rate was 9.2%, 11.9%, 14.1%, and 19.4%, respectively. The mineralization rate only increased by 10.3%

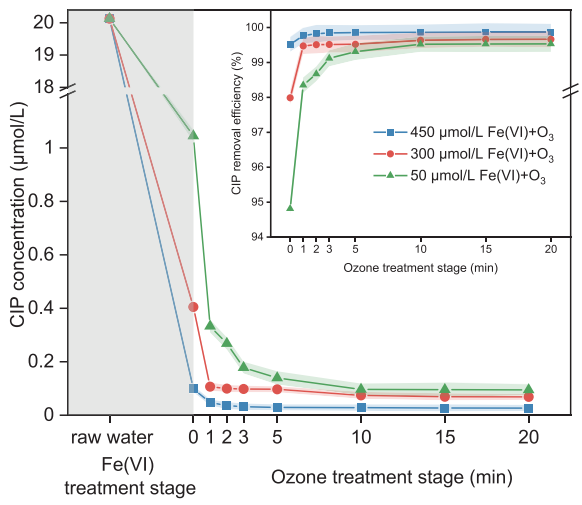

Fig. 2 – Effect of K_2FeO_4 dosage on CIP removal in stepwise oxidation system (CIP = 20 μmol/L, O_3 = 17 mg/L, pH 7 buffer system, 0 min is the water sample after 15 min of K_2FeO_4 treatment).

when the K_2FeO_4 dosage increased from 50 μmol/L to 450 μmol/L. This indicates that although K_2FeO_4 can completely remove the CIP precursors, the mineralization capacity of K_2FeO_4 is weak. The mineralization rate of CIP can be improved very limited by increasing the K_2FeO_4 dosage. However, for the sample treated with 50 μmol/L K_2FeO_4, the mineralization rate of CIP could further increase to 22.6% after 20 min of O_3 reaction (without iron (hydr)oxides). During this process, the mineralization rate of CIP intermediates degraded by O_3 was 13.4%, indicating that O_3 has a stronger ability to mineralize CIP intermediates than K_2FeO_4. With the increase of K_2FeO_4 dosage, the mineralization rate of CIP after 20 min of O_3 treatment (without iron (hydr)oxides) was 22.6%, 25.8%, 29.3%, and 34.2%, respectively. Compared with using K_2FeO_4 treatment alone, the CIP mineralization rate increased by 13.4%, 13.9%, 15.2%, and 14.77%, respectively. It can be concluded that increasing the dosage of K_2FeO_4 can strengthen the pre-oxidation process of CIP to a certain extent, and concentrate the subsequent O_3 oxidation ability on the components which are hardly degraded by K_2FeO_4. Compared with the increase of CIP mineralization rate with 300 μmol/L K_2FeO_4 pretreatment (15.2%), there was a slight de-

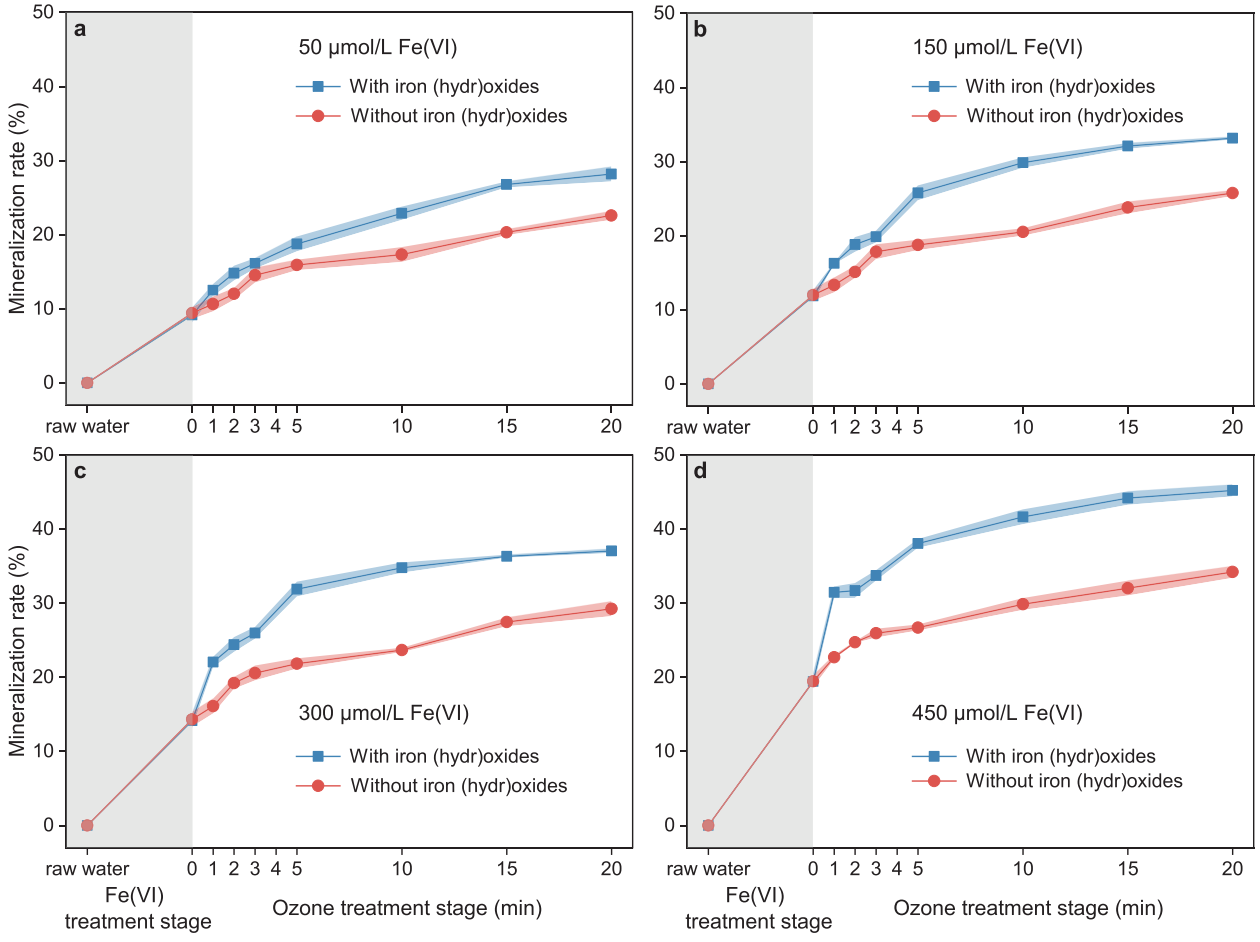

Fig. 3 – Effect of K_2FeO_4 dosage on CIP mineralization rate in ozonation stage with (a) 50 μmol/L K_2FeO_4, (b) 150 μmol/L K_2FeO_4, (c) 300 μmol/L K_2FeO_4, and (d) 450 μmol/L K_2FeO_4 (CIP = 20 μmol/L, O_3 = 17 mg/L, pH 7 buffer system, 0 min is the water sample after 15 min of K_2FeO_4 treatment).

crease with 450 μmol/L K_2FeO_4 pretreatment (14.77%). It may result from the formation of some refractory CIP intermediates after K_2FeO_4 treatment, which even cannot be effectively degraded by O_3 with stronger oxidation capacity. When the dosage of K_2FeO_4 increased from 300 μmol/L to 450 μmol/L, more CIP precursors converted to such refractory intermediates. It explains why the enhancement of CIP mineralization rate decreased slightly.

On the other hand, when the dosage of K_2FeO_4 was 50 μmol/L, the mineralization rate could reach 28.2% by introducing 17 mg/L O_3 for 20 min (in the presence of iron (hydr)oxides). The two different stepwise oxidation treatments had the same reaction conditions except for the presence or absence of iron (hydr)oxides, but there was a significant difference in mineralization rate. Therefore, the increased mineralization rate may result from the further decomposition of O_3 which was catalyzed by the iron (hydr)oxides. With the increase of K_2FeO_4 dosage, the mineralization rate of CIP after 20 min of catalytic ozonation was 28.2%, 33.2%, 37.1%, and 45.2%, respectively. Compared with the treatments without iron (hydr)oxides, the mineralization rate of CIP increased by 5.6%, 7.4%, 7.8%, and 11%, respectively. The advantage of combining K_2FeO_4 pre-oxidation with O_3 treatment became more striking. To summarize, the K_2FeO_4-O_3 combined stepwise oxidation system can firstly utilize K_2FeO_4 to degrade the easily oxidized CIP precursor, and then use iron (hydro)oxides to catalyze ozonation to mineralize CIP intermediate products. Thus, the stepwise oxidative degradation is realized with comprehensive consideration of the properties of pollutants and oxidants.

2.1.2. *Effect of pH on the formation of iron (hydr)oxides*

The pH has an important influence on the decomposition of K_2FeO_4, the formation of the decomposition products, and the ozonation process. Hence the effect of the initial pH on the stepwise oxidation system was investigated (pH = 2, 3, 4, and 5).

It can be seen from Fig. 4 that the initial pH value significantly affected the efficiency of K_2FeO_4 and O_3 treatment. The pH value can affect the decomposition rate of K_2FeO_4. In addition, the self-decomposition of K_2FeO_4 in solution will in turn increase the pH value of the aqueous solution, which may affect the formation and structures of the reduction products. The treatment effect using K_2FeO_4 alone was optimal with an initial pH of 3 (37.98%) and worst at pH 2 (1.91%). This may be attributed to the rapid decomposition of K_2FeO_4 at pH 2, which failed to apply its oxidizing power to the contaminants ($FeO_4^{2-} + 8H^+ + 3e^- \rightarrow Fe^{3+} + 4H_2O$) (Eng et al., 2006; Wood, 2002). The pH value fluctuated less (pH = 2.21) after the addition of K_2FeO_4 at an initial pH of 2. At this pH, it was difficult to form iron (hydr)oxides for flocculation, so the treatment effect was further weakened. The pH of the solution raised rapidly (pH = 7.02) after the addition of K_2FeO_4 at an initial pH of 3. Compared to the condition with an initial pH of 2, in addition to the oxidation capacity of K_2FeO_4, it can also use the flocculation of reduction products to remove pollutants. At an initial pH of 4–5, the pH of the water samples would raise to alkaline (pH 9–10.32) during the decomposition and reduction of K_2FeO_4. As the pH value raised, the oxidizing capacity of K_2FeO_4 decreased, so the mineralization capacity decreased compared to that with an initial pH of 3.

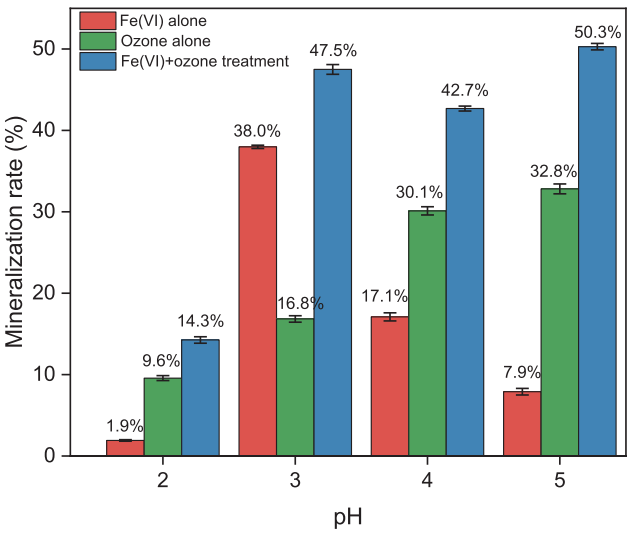

Fig. 4 – Effect of initial pH value on mineralization rate using different treatments (K_2FeO_4 = 450 μmol/L, CIP = 20 μmol/L, O_3 = 17 mg/L, t = 15 min).

Fig. 4 also indicates that the treatment effect of O_3 treatment alone increased with increasing pH, which may be ascribed to the ability of OH^- to act as an initiator for radical chain reactions (Nemati Sani et al., 2019). It is reported that O_3 is easier to decompose and generate ·OH under alkaline conditions (An et al., 2020). With the rise of pH value, the concentration of OH^- increased and more ·OH was generated. Therefore, the free radical chain reactions were enhanced, which promoted the mineralization rate of CIP.

The combination of K_2FeO_4 and O_3 was obviously more effective than the other two treatments, and achieved an optimal mineralization rate of 50.3% at an initial pH of 5. At this pH value, the CIP mineralization rate was only 7.9% and 32.8% after K_2FeO_4 and O_3 treatment alone, respectively. Compared with the K_2FeO_4 treatment, the mineralization rate remarkably increased by 42.4% after combining with O_3 treatment, which was also notably higher than the single O_3 treatment. Under this pH condition, the pre-oxidation effect of K_2FeO_4 was lower than that at pH 3–4. Based on the previous conclusion, it is speculated that partial oxidation capacity of O_3 was wasted in degrading the easily degradable precursors of pollutants. As a result, the mineralization effect of CIP decreased. However, the enhancement of mineralization rate after combined use of O_3 was much greater than that under other pH conditions, which may result from the elevated pH of the water sample after K_2FeO_4 treatment. The increased pH promoted the decomposition of O_3 to produce more ·OH to strengthen the mineralization effect of CIP. On the other hand, we speculate that the iron (hydr)oxides were more readily converted into the components that can catalyze ozonation at this pH value. As a result, the effect of catalytic ozonation was strengthened.

To explored the effect of pH on iron (hydr)oxides, we further used the pH buffer system (pH = 6, 7, and 8) to control the pH variation during the reaction to exclude the effect of pH changes on ozonation.

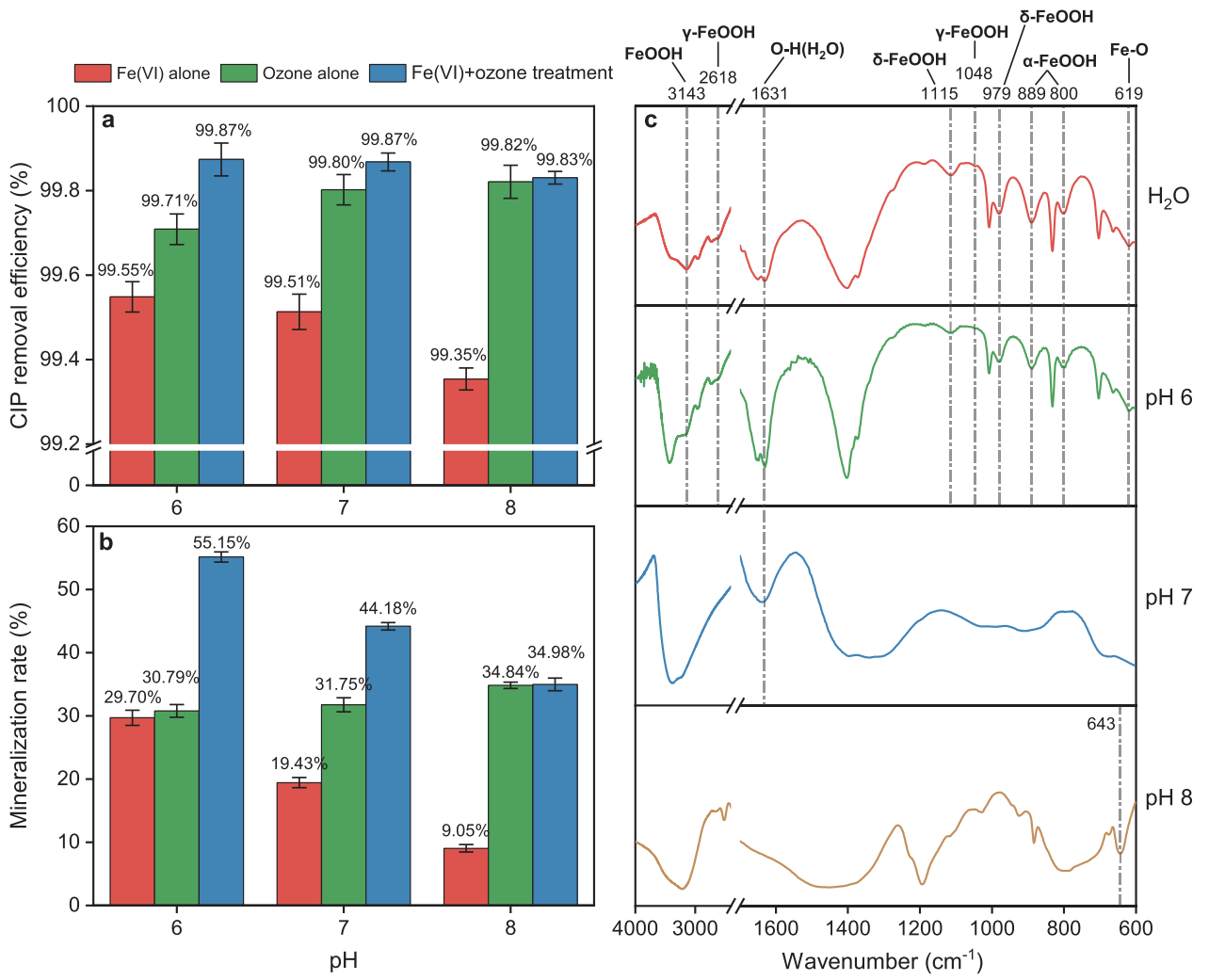

Fig. 5 – (a) Removal efficiency and (b) mineralization rate of CIP by three different treatments in the buffer systems of pH 6, 7, and 8 (K_2FeO_4 = 450 μmol/L, CIP = 20 μmol/L, O_3 = 17 mg/L, t = 15 min), (c) FT-IR spectra of iron (hydr)oxides under different conditions.

As demonstrated in Fig. 5a, all three treatments were able to remove more than 99% of the CIP under all pH buffer conditions. Fig. 5b shows that the effect of O_3 treatment alone increased with increasing pH (mineralization rate increased from 30.8% to 34.8%), while the effect of K_2FeO_4 treatment alone and stepwise oxidation treatment decreased as pH increased (mineralization rate decreased from 29.7% and 55.2% to 9.1% and 35.0%, respectively). As the pH increased, the elevated content of OH^- improved the decomposition rate of O_3. As a consequence, the ·OH was more readily produced, thus improving the effectiveness of O_3 treatment alone.

The pH value of the aqueous solution can not only influence the formation of free radicals by affecting the decomposition of O_3, but also be an important factor in determining the surface hydroxyl charge properties of the substrate at the oxide/water interface. Due to the protonation and deprotonation processes, the surface charge of CIP is largely influenced by the solution pH. The pKa values of CIP are 5.90 ± 0.15 and 8.89 ± 0.11, so it can exist in the form of cations (pH ≤ 5.90 ± 0.15, positively charged N atom), amphoteric ions (5.90 ± 0.15 ≤ pH ≤ 8.89 ± 0.11), and anions (pH ≥ 8.89 ± 0.11, negatively charged carboxyl group) in water (Genç and Dogan, 2013). For antibiotics with amphoteric properties, the solution pH can affect the morphological distribution of their molecular and ionic forms as well as their surface charge properties, thereby generate attractive or repulsive forces between different antibiotic species, and ultimately affect the degradation efficiency (Zhang and Ma, 2008). In the selected pH buffer systems, the pH was controlled between 6 and 8. Under this condition, CIP existed in the form of amphoteric ions, which excluded the effect of pH on the surface charge of CIP.

On the other hand, the charge state of the surface hydroxyl groups depends on whether the solution pH is below or above the point of zero charge (pH_{pzc}) of the catalyst. When the solution pH is close to the pH_{pzc}, most surface hydroxyl groups exist in a neutral state. When the solution pH is below or above the pH_{pzc}, the protonation or deprotonation occurs on the oxide surface, respectively (Zhang et al., 2008). Consequently, the adsorption capacity and catalytic activity of the catalyst are

changed. Because O_3 has both nucleophilic and electrophilic sites (Zhang and Ma, 2008), it can bind with surface hydroxyl groups (H and O of surface hydroxyl are electrophilic and nucleophilic, respectively). The decomposition of the binding substances produces the surface HO_2^-, which can react with another O_3 molecule to form ·OH and $O_2\cdot^-$. $O_2\cdot^-$ can further react with O_3 to finally generate another ·OH. The surface protonation or deprotonation of the iron (hydr)oxides can affect the formation of ·OH by influencing the binding of O_3 to the surface hydroxyl groups. It has been reported that the pH_{pzc} of α-FeOOH is about 9 (Gaboriaud and Ehrhardt, 2003), and the pH_{pzc} of γ-FeOOH is about 7–8 (Botella and Lefèvre, 2022), so the surface of the iron (hydr)oxides are protonated at pH 6. Because the protonation can cause the nucleophilic property of O in the surface hydroxyl to be weaker than those in the neutral hydroxyl (Wang and Bai, 2017), the protonation of the surface hydroxyl is not conducive to its surface binding with O_3. Compared with the conditions at pH 7 and 8, the interaction between surface hydroxyl and O_3 was weakened at pH 6, and the efficiency of catalyzing O_3 decomposition to produce ·OH was reduced. Therefore, it was speculated that the mineralization rate of CIP was the lowest at pH 6. However, the experimental results (Fig. 5b) show that the mineralization rate of CIP reached a maximum of 55.2% in a buffer system with a pH of 6. This phenomenon that the effect of ozonation in stepwise oxidation system increased with decreasing pH contradicted with the relationship between O_3 decomposition and pH in O_3 treatment alone. It suggests that in addition to the direct ozonation and the oxidation by ·OH originated from O_3 decomposition induced by OH^-, the catalytic ozonation also existed and dominated this process. Besides, according to our previous analysis, the interaction between surface hydroxyl and O_3 was weakened at pH 6, resulting in the decline of the treatment effect, which also contradicted with the fact that the mineralization rate of CIP was optimal at this pH value in stepwise oxidation system. Therefore, it is further proved that more iron (hydr)oxides with catalytic components were produced at this pH than at other pH values. On the other hand, the effect of O_3 treatment alone at pH 8 was very close to that of stepwise oxidation treatment. This may result from two reasons. Firstly, the surface of the catalytic components in iron (hydr)oxides was protonated or deprotonated under this condition, which hindered the interaction of surface hydroxyl groups with O_3 and inhibited the catalysis (Zhang and Ma, 2008). Secondly, when pH was equal to 8, the content of the catalytic components in iron (hydr)oxides formed by the reduction of K_2FeO_4 decreased, resulting in a reduced catalytic O_3 capacity. Based on the above phenomena, it can be concluded that the formation of the catalytic components in iron (hydr)oxides is affected by pH value. It means that in the process of K_2FeO_4 treatment, the pH value of the aqueous solution will influence the K_2FeO_4 reduction products. Higher pH conditions will make iron (hydr)oxides convert into $Fe(OH)_3$, which weakens the catalytic effect.

The iron (hydr)oxides formed in water or in the buffer systems with pH 6, 7, and 8 were characterized and analyzed by FT-IR technique. The composition of the products was deduced by the structure of the functional groups. By comparing the effect of pH on the components structures, its influence on the stepwise oxidation system was further explained.

As can be seen from Fig. 5c, a broad absorption peak of water appeared around 3400 cm^{-1}. A strong and sharp absorption peak was observed at 3143 cm^{-1}, which can be ascribed to the stretching vibration of the surface hydroxyl group of FeOOH (Yuan et al., 2016). The characteristic peak at 2618 cm^{-1} can be attributed to the υ(FeO–H) stretching vibration on γ-FeOOH surface (Zhang et al., 2008). The absorption peak at 1630–1700 cm^{-1} can be attributed to the δ(O–H) bending vibration of the adsorbed H_2O molecules (Oputu et al., 2015), so the characteristic absorption peak at 1631 cm^{-1} was the O–H bond in H_2O molecules absorbed on the self-decomposition products of K_2FeO_4. The absorption peaks at 1115 cm^{-1} and 979 cm^{-1} in Fig. 5c are similar to the characteristic absorption peaks of δ-FeOOH (1124 and 975 cm^{-1}) mentioned in previous literature (Huang et al., 2021), and the absorption peak at 1048 cm^{-1} is close to the characteristic absorption peak of γ-FeOOH (Smith et al., 1998). It indicates that different forms of FeOOH may exist simultaneously in the self-decomposition products of K_2FeO_4. Various FeOOH can transform into each other and act together as catalysts for O_3. The strong and sharp absorption peaks at 889 cm^{-1} and 800 cm^{-1} are typical δ(FeO–H) bending vibration peaks in α-FeOOH (Wang et al., 2018). It confirms that FeOOH is indeed present in the self-decomposition products of K_2FeO_4 (Yan et al., 2016). The peak at 619 cm^{-1} represented the stretching vibration of the Fe–O bond (Yuan et al., 2016). Based on the above conclusions, iron (hydr)oxides are composed of various FeOOH. Because different forms of FeOOH can convert into each other, various forms of FeOOH may co-exist in the self-decomposition product of K_2FeO_4. The vibration peak at 1631 cm^{-1} also confirms that the H_2O molecules can be adsorbed on iron (hydr)oxides surface. The dissociation of the adsorbed H_2O molecules will result in the hydroxylation on iron (hydr)oxides surface. These hydroxyls can release protons and act as Brönsted acid sites. The adsorbed H_2O molecules are desorbed to form metal cations and coordinated unsaturated oxygen, which can act as Lewis acid and Lewis base, respectively. The FeO–H bond on FeOOH surface is beneficial to the interaction between surface hydroxyl groups and O_3 in water. As a dipole molecule, O_3 has both nucleophilic sites and electrophilic sites, which can bind with both H (electrophilic) atoms and O (nucleophilic) atoms of the surface hydroxyl groups in the interaction process. This combination will promote O_3 decomposition, thereby promoting the generation of ·OH (Zhang et al., 2008).

Fig. 5c also demonstrates that iron (hydr)oxides showed significant differences in the buffer systems at different pH values. In the buffer system with pH equal to 6, the positions of the vibration peaks of iron (hydr)oxides fluctuated little, indicating the presence of various forms of FeOOH and other iron oxides. Under the buffer condition of pH 7, the characteristic absorption peaks of δ-FeOOH (1115 cm^{-1} and 979 cm^{-1}) disappeared. Besides, the δ(Fe–OH) bending vibration peak of α-FeOOH (889 cm^{-1} and 800 cm^{-1}) broadened, which indicated that the structures and species of FeOOH decreased. However, the O–H bonds of H_2O molecules adsorbed on the surface still existed, indicating that the remaining FeOOH structures can still effectively adsorb H_2O and catalyze O_3 to generate ·OH. In the buffer system with pH 8, the characteristic peaks related to FeOOH is not obvious. Nevertheless, there was a remarkable absorption peak at 643 cm^{-1}, which was attributed to the ab-

sorption peak of the Fe–O bond in iron oxide (Wang et al., 2018). It indicated that iron (hydr)oxides were still the main component, but the reduced structures and species of FeOOH significantly affected the effect of catalytic ozonation. The peak of the adsorbed water molecular near 1631 cm^{-1} disappeared, indicating a decrease of the chemisorption water formed on iron (hydr)oxide surface. It also proved that the Lewis acid sites on the surface were reduced (Yang et al., 2010), so the catalytic effect of iron (hydr)oxides on ozonation in water was weakened apparently. This was consistent with the lowest mineralization rate of CIP in the buffer system with pH 8 in our experiment. At this pH, the amount of the characteristic peaks decreased compared with the peaks in pure water, which also indicated the decrease of the components with catalytic ozonation capacity. The FTIR results further verified the hypothesis that pH can affect the composition of the iron (hydr)oxides.

2.1.3. *Effect of pre-oxidation time of K_2FeO_4 on the formation of iron (hydr)oxides*

To investigate the effect of the pre-oxidation time of K_2FeO_4 on the formation of the iron (hydr)oxides, we compared the treatment effect of three different modes with that of O_3 treatment alone: (1) K_2FeO_4 pre-oxidation until the complete reduction of K_2FeO_4, then in combination with O_3 (Mode 1), (2) simultaneous treatment of K_2FeO_4 and O_3 (without K_2FeO_4 pre-oxidation, Mode 2), (3) K_2FeO_4 pre-oxidation for 10 sec and then in combination with O_3 (Mode 3). The mineralization rate and pH changes are shown in Fig. 6a-b.

Fig. 6a shows that the mineralization rate of CIP after Mode 1 treatment was higher than the other three treatments. During the process of O_3 treatment alone, the pH value of the aqueous solution decreased continuously (Fig. 6b). This is because O_3 can use its own oxidation to destroy the unsaturated bond of CIP to generate ozonide. The spontaneous splitting of the ozonide produced carboxyl compounds and amphoteric ions with acidic/basic groups. The amphoteric ions with acidic/basic groups were unstable and can be decomposed into acids and aldehydes, which lowered the pH of the solution. The decreased pH of the aqueous solution inhibited the generation of ·OH from O_3 decomposition and led to direct ozonation. Therefore, the mineralization rate reached 31.3% after 10 min of O_3 treatment alone and increased slightly after that. After pre-oxidation with K_2FeO_4, the pH increased rapidly to above 10. Differences in pH changes were observed using different pre-oxidation time. The pH in Mode 1 decreased from 10.32 to 7.12, while the pH of the other two experimental groups decreased from 10.22 to 9.59. This may result from that the K_2FeO_4 was not fully reduced and constantly hydrolyzed to produce ·OH in the process of combined use with O_3 to neutralize the acidic products generated by oxidation, so that the pH changed little. The complete pre-oxidation of K_2FeO_4 combined with O_3 treatment for 30 min made the mineralization rate of CIP reach 54.9%. For comparison, the mineralization rate of the other two experimental groups was 50.1% (Mode 2) and 50.5% (Mode 3), respectively. In this process, the pH in the O_3 treatment stage of Mode 1 was lower than that of the other two experimental groups, which inhibited O_3 generating more ·OH. However, the mineralization rate of CIP had been improved. Therefore, it was speculated that the pre-oxidation time of K_2FeO_4 would affect the catalysis of iron (hydr)oxides.

In the pH-buffered system, the influence of K_2FeO_4 pre-oxidation time on iron (hydr)oxides formation was further investigated. The treatment effects after Mode 1 treatment, Mode 2 treatment, and O_3 treatment alone were compared. Fig. 6c clearly demonstrates that the mineralization rate of CIP after Mode 1 treatment was significantly higher than those after the other two treatments. The mineralization rate of CIP reached 57.4% after complete K_2FeO_4 pre-oxidation combined with 30 min O_3 treatment. In contrast, the mineralization rate after O_3 treatment alone and Mode 2 treatment was 36.3% and 51.4%, respectively. In buffer system with pH 6, the oxidation capacity of K_2FeO_4 alone resulted in a CIP mineralization rate of 29.7%. Mode 1 treatment showed a higher mineralization rate than Mode 2 treatment. In this process, the effect of pH on ozonation ability was excluded. The only difference between the two treatment modes was the pre-oxidation time of K_2FeO_4. Therefore, the different effects can be attributed to different pre-oxidation time of K_2FeO_4, which resulted in different catalytic effects of iron (hydr)oxides. According to this analysis, in Mode 2 treatment (without the K_2FeO_4 pre-oxidation process), K_2FeO_4 was in direct contact with O_3, hence the reduction process of K_2FeO_4 was influenced by ozonation. The low-valent iron (Fe(III) and Fe(II)) produced by the reduction of K_2FeO_4 can be oxidized by O_3 and free radicals (O_2·, ·OH), which changed the structure and composition of the iron (hydr)oxides. Furthermore, the components with catalytic ozonation effect in the iron (hydr)oxides were also decreased, thus the subsequent catalytic ozonation ability was weakened. This means that the pre-oxidation stage of K_2FeO_4 can avoid the decrease of the catalytic components in iron (hydr)oxides caused by ozonation.

2.2. *Inference of CIP degradation products and pathways*

2.2.1. *Identification of CIP degradation products by stepwise oxidation system*

Water samples were selected for analysis by FT-ICR-MS using K_2FeO_4 treatment alone (5 min, the moment when the purple color disappeared), O_3 treatment alone (5, 15 min), and K_2FeO_4–O_3 stepwise oxidation treatment (5, 15 min). The results of the mass spectrometry after 15 min stepwise oxidation treatment are shown in Appendix A **Fig. S2**.

Based on the oxidation products reported in previous literature, the structure of the intermediate products shown in the mass spectrometry was speculated. The results are listed in Appendix A **Table S1**. P3 was detected during the whole process of K_2FeO_4 treatment alone and in the first 5 min of O_3 treatment alone. This indicated that P3 was a primary oxidation product in the process of ozonation and will be further oxidized over time. As a contrast, more ·OH was generated in the stepwise oxidation process. Because of the faster reaction rate, P3 was already degraded or converted to other forms within 5 min in the stepwise oxidation system. However, the oxidation performance of K_2FeO_4 was weaker than that of the other two treatments, hence P3 was the final decomposition product in the process of K_2FeO_4 treatment alone. P5 was only detected in the first 5 min of K_2FeO_4 treatment alone and O_3 treatment

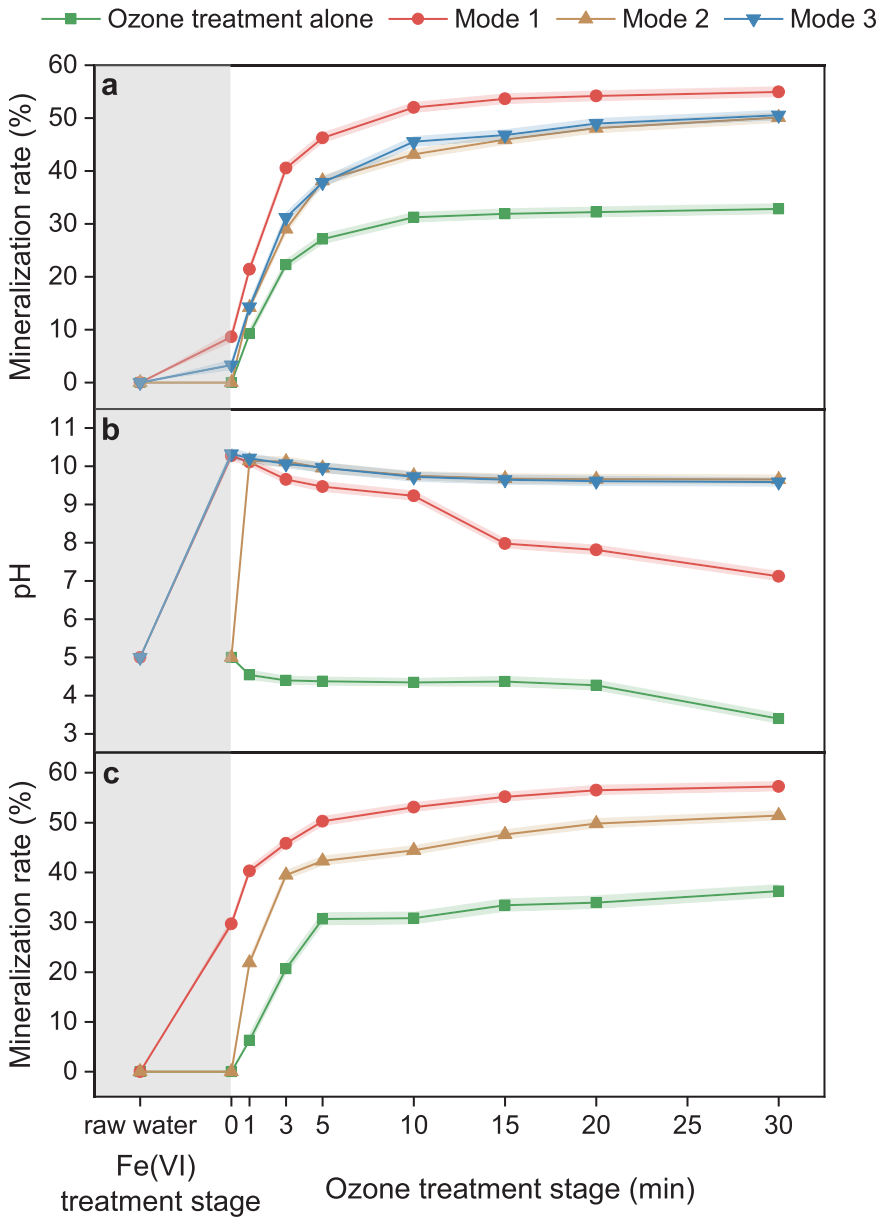

Fig. 6 – (a) Mineralization rate and (b) pH changes of water samples during the oxidation process of four different treatments with an initial pH of 5 (K_2FeO_4 = 450 μmol/L, CIP = 20 μmol/L, O_3 = 17 mg/L), (c) mineralization rate of water samples during the oxidation process of three different treatments in pH 6 buffer system (K_2FeO_4 = 450 μmol/L, CIP = 20 μmol/L, O_3 = 17 mg/L).

alone, demonstrating that P5 was a primary oxidation product of the oxidation process and was easily degraded. P6 and P10 were detected during the whole process of K_2FeO_4 treatment alone and in the first 5 min of O_3 treatment alone and stepwise oxidation treatment, indicating that P6 and P10 were the final products for K_2FeO_4 treatment alone. However, due to the stronger oxidation performance of O_3 treatment and stepwise oxidation treatment, P6 and P10 can be further oxidized and degraded over time. The disappearance of P6 and P10 after 15 min of O_3 treatment alone indicated that P6 and P10 can be effectively degraded depending on the oxidation capacity of O_3. P11 and P12 were only detected during the whole process of stepwise oxidation treatment, and the products with the destroyed quinolone group appeared. It indicated that K_2FeO_4 treatment alone or O_3 treatment alone had difficulty in degrading the quinolone group of CIP. In the study of verifying the oxidation effect of ·OH on CIP, Dewitte et al. (2008) found that there were significant differences in the quinolone groups of the oxidation products with and without ·OH scavenger (t-BuOH). In the absence of t-BuOH, reaction products with the broken quinolone moiety were observed. While in the presence of t-BuOH, the quinolone ring remained intact. It proved

that the destruction of the quinolone ring in CIP mainly resulted from the oxidative ability of ·OH.

2.2.2. Reaction pathway analysis for the degradation of CIP in the stepwise oxidation system

Based on the identification results and previous studies, the inferred reaction pathways of O_3 treatment alone and stepwise oxidation treatment are shown in Appendix A **Fig. S3** and **Fig. S4**, respectively. OH one-electron can oxidize the secondary amine of the piperazine substituent to generate an N-centered radical cation (Mahdi-Ahmed and Chiron, 2014). After hydration, the radical cation was further oxidized by O_3 and ·OH to form P1. Subsequently, the piperazine ring in P1 was cleaved and formed the ketone derivatives P4 and P4′ after losing the C–O bond. The carbonyl group (–CHO) may remain on the N atom of aniline or alkyl amine. The intermediate product P6 was detected in the first 5 min of the stepwise oxidation treatment and could be attributed to the defluorination of P4. ·OH as a strong oxidant and an electrophilic reagent, is easily added to the unsaturated bond of the benzene ring (Wang and Chu, 2016), which would be further converted to P2, P3, and P5. The C=O group in P4 and P4′ was cleaved from the N atom to form P7. P7 was further oxidized by ·OH in the catalytic ozonation process and formed P8 with ketone groups by losing $–NH_2$ and $–CH_3$. The remaining piperazine of P8 was further degraded to amine after removing the carbonyl group on the secondary amine-N atom, thus forming P9. At this time, the piperazine substituents of CIP were completely destroyed. On the one hand, ·OH attacked the quinolone part of P9 on the C=C double bond adjacent to the –COOH group (Chen and Wang, 2021), the unsaturated double bond was easily broken by oxidation. The quinolone group was destroyed and the cyclopropyl on the N atom was lost, hence P12 was formed. On the other hand, P9 could form P10 by losing the carboxyl group (–COOH). The oxidation of the quinolone fraction and the loss of the fluorine atom in P10 produced the intermediate P11 (Mohan and Balakrishnan, 2021). P11 and P12 were detected only in the stepwise oxidation treatment, with the complete destruction of the piperazine ring and partial ring-opening of the quinolone structure, which further proved that K_2FeO_4 or O_3 treatment alone cannot effectively destroy the quinolone ring structure of CIP. In contrast, the stepwise oxidation system can effectively destroy the structures of piperazine and quinolone groups in CIP molecules and realize effective degradation.

3. Conclusions

Although K_2FeO_4 or O_3 treatment alone can effectively degrade more than 99% of CIP, the mineralization rate after each individual treatment was unsatisfied. The stepwise oxidation system of K_2FeO_4 combined with O_3 effectively improved the mineralization rate of CIP. Iron (hydr)oxides played a catalytic role for ozonation in the stepwise oxidation system. The pH value can influence the amount and types of the components in iron (hydr)oxides with catalytic ozonation effect. The K_2FeO_4 pre-oxidation stage produced more iron (hydr)oxides with catalytic components. Moreover, it can avoid the decrease of the catalytic components in iron (hydr)oxides caused by the oxidation of O_3 and free radicals. According to FT-ICR-MS analysis, the intermediate products of CIP degradation were identified. It was found that the destroyed quinolone ring structure only appeared in the stepwise oxidation system. The oxidative degradation product $C_{10}H_9FN_2O_4$ ($m/z = 239.04$) was only observed in the stepwise oxidation system.

In this work, the factors affecting the formation and transformation of the iron (hydr)oxides were explored from the perspective of the iron (hydr)oxides. The findings of this work laid a foundation for improving the degradation effect of the refractory pollutants by the stepwise oxidation system. However, the mineralization of CIP was still incomplete, which was mainly attributed to the low content of the catalytic ozonation components in iron (hydr)oxides. Therefore, further work is needed to promote the transformation of the K_2FeO_4 reduction products to the iron (hydr)oxides with more catalytic ozonation components.

Declaration of Competing Interest

The authors declare that they have no known competing financial interests or personal relationships that could have appeared to influence the work reported in this paper.

Acknowledgments

This work was supported by the National Natural Science Foundation of China (No. 51878394) and the Introduction and Cultivation Plan for Young Innovative Talents of Colleges and Universities by the Education Department of Shandong Province.

Appendix A Supplementary data

Supplementary material associated with this article can be found, in the online version, at doi:10.1016/j.jes.2022.12.018.

REFERENCES

An, W.J., Tian, L.Y., Hu, J.S., Liu, L., Cui, W.Q., Liang, Y.H., 2020. Efficient degradation of organic pollutants by catalytic ozonation and photocatalysis synergy system using double-functional MgO/g-C_3N_4 catalyst. Appl. Surf. Sci. 534, 147518.

Dewitte, B., Dewulf, J., Demeestere, K., Van De Vyvere, V., De Wispelaere, P., Van Langenhove, H., 2008. Ozonation of ciprofloxacin in water: HRMS identification of reaction products and pathways. Environ. Sci. Technol. 42, 4889–4895.

Botella, R., Lefèvre, G., 2022. A deep look into the diverse surface speciation of the mono-molybdate/lepidocrocite system by ATR-IR and polarized ATR-IR spectroscopy. Colloids Surf., A 647, 129065.

Breazeal, M.V., Novak, J.T., Vikesland, P.J., Pruden, A., 2013. Effect of wastewater colloids on membrane removal of antibiotic resistance genes. Water Res. 47, 130–140.

Chen, H., Wang, J.L., 2019. Catalytic ozonation of sulfamethoxazole over Fe_3O_4/Co_3O_4 composites. Chemosphere 234, 14–24.

Chen, H., Wang, J., 2021. MOF-derived Co_3O_4-C@FeOOH as an efficient catalyst for catalytic ozonation of norfloxacin. J. Hazard. Mater. 403, 123697.
De Witte, B., Van Langenhove, H., Demeestere, K., Saerens, K., De Wispelaere, P., Dewulf, J., 2010. Ciprofloxacin ozonation in hospital wastewater treatment plant effluent: effect of pH and H_2O_2. Chemosphere 78, 1142–1147.
Eng, Y.Y., Sharma, V.K., Ray, A.K., 2006. Ferrate(VI): green chemistry oxidant for degradation of cationic surfactant. Chemosphere 63, 1785–1790.
Gaboriaud, F., Ehrhardt, J.-J., 2003. Effects of different crystal faces on the surface charge of colloidal goethite (α-FeOOH) particles: an experimental and modeling study. Geochim. Cosmochim. Acta 67, 967–983.
Genç, N., Dogan, E.C., 2013. Adsorption kinetics of the antibiotic ciprofloxacin on bentonite, activated carbon, zeolite, and pumice. Desalin. Water Treat. 53, 785–793.
Han, Q., Dong, W.Y., Wang, H.J., Ma, H., Gu, Y.R., Tian, Y., 2019. Degradation of tetrabromobisphenol A by a ferrate(VI)-ozone combination process: advantages, optimization, and mechanistic analysis. RSC Adv. 9, 41783–41793.
Han, Q., Wang, H.J., Dong, W.Y., Liu, T.Z., Yin, Y.L., 2013. Formation and inhibition of bromate during ferrate(VI) – Ozone oxidation process. Sep. Purif. Technol. 118, 653–658.
Huang, Y., Su, M.H., Chen, D.Y., Zhu, L.Q., Pang, Y.X., Chen, Y.H., 2021. Highly-efficient and easy separation of hexahedral sodium dodecyl sulfonate/δ-FeOOH colloidal particles for enhanced removal of aqueous thallium and uranium ions: synergistic effect and mechanism study. J. Hazard. Mater. 402, 123800.
Iakovides, I.C., Michael-Kordatou, I., Moreira, N.F.F., Ribeiro, A.R., Fernandes, T., Pereira, M.F.R., et al., 2019. Continuous ozonation of urban wastewater: removal of antibiotics, antibiotic-resistant Escherichia coli and antibiotic resistance genes and phytotoxicity. Water Res. 159, 333–347.
Kim, D., Nguyen, L.N., Oh, S., 2020. Ecological impact of the antibiotic ciprofloxacin on microbial community of aerobic activated sludge. Environ. Geochem. Health 42, 1531–1541.
Lee, Y., Kissner, R., Von Gunten, U., 2014. Reaction of ferrate(VI) with ABTS and self-decay of ferrate(VI): kinetics and mechanisms. Environ. Sci. Technol. 48, 5154–5162.
Li, B.B., Li, C.G., Qu, R.J., Wu, N.N., Qi, Y.M., Sun, C., et al., 2020. Effects of common inorganic anions on the ozonation of polychlorinated diphenyl sulfides on silica gel: kinetics, mechanisms, and theoretical calculations. Water Res. 186, 116358.
Li, G.T., Wang, N.G., Liu, B.T., Zhang, X.W., 2009. Decolorization of azo dye Orange II by ferrate(VI)–hypochlorite liquid mixture, potassium ferrate(VI) and potassium permanganate. Desalination 249, 936–941.
Li, X.F., Chen, W.Y., Ma, L.M., Wang, H.W., Fan, J.H., 2018. Industrial wastewater advanced treatment via catalytic ozonation with an Fe-based catalyst. Chemosphere 195, 336–343.
Ling, W.C., Ben, W.W., Xu, K., Zhang, Y., Yang, M., Qiang, Z.M., 2018. Ozonation of norfloxacin and levofloxacin in water: specific reaction rate constants and defluorination reaction. Chemosphere 195, 252–259.
Liu, J., Zhang, Z.H., Chen, Q.H., Zhang, X.H., 2018. Synergistic effect of ferrate (VI)-ozone integrated pretreatment on the improvement of water quality and fouling alleviation of ceramic UF membrane in reclaimed water treatment. J. Membr. Sci. 567, 216–227.
Liu, Z.G., Sun, P.Z., Pavlostathis, S.G., Zhou, X.F., Zhang, Y.L., 2013. Adsorption, inhibition, and biotransformation of ciprofloxacin under aerobic conditions. Bioresour. Technol. 144, 644–651.
Mahdi-Ahmed, M., Chiron, S., 2014. Ciprofloxacin oxidation by UV-C activated peroxymonosulfate in wastewater. J. Hazard. Mater. 265, 41–46.
Mohan, S., Balakrishnan, P., 2021. Kinetics of ciprofloxacin removal using a sequential two-step ozonation-biotreatment process. Environ. Technol. Innovation 21, 101284.
Nemati Sani, O., Navaei fezabady, A.A., Yazdani, M., Taghavi, M., 2019. Catalytic ozonation of ciprofloxacin using γ-Al_2O_3 nanoparticles in synthetic and real wastewaters. J. Water Process. Eng. 32, 100894.
Von Gunten, U., Oliveras, Y., 1998. Advanced oxidation of bromide-containing waters: bromate formation mechanisms. Environ. Sci. Technol. 32, 63–70.
Oputu, O., Chowdhury, M., Nyamayaro, K., Fatoki, O., Fester, V., 2015. Catalytic activities of ultra-small β-FeOOH nanorods in ozonation of 4-chlorophenol. J. Environ. Sci. 35, 83–90.
Porras, J., Bedoya, C., Silva-Agredo, J., Santamaria, A., Fernandez, J.J., Torres-Palma, R.A., 2016. Role of humic substances in the degradation pathways and residual antibacterial activity during the photodecomposition of the antibiotic ciprofloxacin in water. Water Res 94, 1–9.
Prucek, R., Tucek, J., Kolarik, J., Filip, J., Marusak, Z., Sharma, V.K., et al., 2013. Ferrate(VI)-induced arsenite and arsenate removal by in situ structural incorporation into magnetic iron(III) oxide nanoparticles. Environ. Sci. Technol. 47, 3283–3292.
Prucek, R., Tucek, J., Kolarik, J., Huskova, I., Filip, J., Varma, R.S., et al., 2015. Ferrate(VI)-prompted removal of metals in aqueous media: mechanistic delineation of enhanced efficiency via metal entrenchment in magnetic oxides. Environ. Sci. Technol. 49, 2319–2327.
Sharma, V.K., Zboril, R., Varma, R.S., 2015. Ferrates: greener oxidants with multimodal action in water treatment technologies. Acc. Chem. Res. 48, 182–191.
Smith, E.R.G., Naidu, R., Alston, A., 1998. Arsenic in the Soil Environment. Academic Press.
Wang, C., Li, A.M., Shuang, C.D., 2018. The effect on ozone catalytic performance of prepared-FeOOH by different precursors. J. Environ. Manag. 228, 158–164.
Wang, J.L., Bai, Z.Y., 2017. Fe-based catalysts for heterogeneous catalytic ozonation of emerging contaminants in water and wastewater. Chem. Eng. J. 312, 79–98.
Wang, J.L., Chen, H., 2020. Catalytic ozonation for water and wastewater treatment: recent advances and perspective. Sci. Total Environ. 704, 135249.
Wang, J.L., Chu, L.B., 2016. Irradiation treatment of pharmaceutical and personal care products (PPCPs) in water and wastewater: an overview. Radiat. Phys. Chem. 125, 56–64.
Wang, J.L., Xu, L.J., 2012. Advanced oxidation processes for wastewater treatment: formation of hydroxyl radical and application. Crit. Rev. Environ. Sci. Technol. 42, 251–325.
Wang, Y.F., Wang, N., Li, M., Bai, M.M., Wang, H.B., 2022. Potassium ferrate enhances ozone treatment of pharmaceutical wastewaters: oxidation and catalysis. J. Water Process. Eng. 49, 103055.
Wood, R.H., 2002. The heat, free energy and entropy of the ferrate(VI) ion. J. Am. Chem. Soc. 80, 2038–2041.
Yan, W.J., Zhou, J.M., Liu, H., Chen, R.F., Zhang, Y.F., Wei, Y., 2016. Formation of goethite and magnetite rust via reaction with Fe(II). J. Electrochem. Soc. 163, C289–C295.
Yang, L., Hu, C., Nie, Y.L., Qu, J.H., 2010. Surface acidity and reactivity of β-FeOOH/Al_2O_3 for pharmaceuticals degradation with ozone: in situ ATR-FTIR studies. Appl. Catal., B 97, 340–346.
Yuan, L., Shen, J.M., Chen, Z.L., Guan, X.H., 2016. Role of Fe/pumice composition and structure in promoting ozonation reactions. Appl. Catal., B 180, 707–714.
Yuan, L., Shen, J.M., Yan, P.W., Zhang, J., Wang, Z., Zhao, S.X., et al., 2019. Catalytic ozonation of 4-chloronitrobenzene by goethite and Fe^{2+}-modified goethite with low defects: a comparative study. J. Hazard. Mater. 365, 744–750.

Zhang, T., Li, C.J., Ma, J., Tian, H., Qiang, Z.M., 2008. Surface hydroxyl groups of synthetic α-FeOOH in promoting ·OH generation from aqueous ozone: property and activity relationship. Appl. Catal., B 82, 131–137.

Zhang, T., Ma, J., 2008. Catalytic ozonation of trace nitrobenzene in water with synthetic goethite. J. Mol. Catal. A: Chem. 279, 82–89.

Zhang, X.X., Li, R.P., Jia, M.K., Wang, S.L., Huang, Y.P., Chen, C.C., 2015. Degradation of ciprofloxacin in aqueous bismuth oxybromide (BiOBr) suspensions under visible light irradiation: a direct hole oxidation pathway. Chem. Eng. J. 274, 290–297.

Zheng, Q., Wu, N.N., Qu, R.J., Albasher, G., Cao, W.M., Li, B.B., et al., 2021. Kinetics and reaction pathways for the transformation of 4-*tert*-butylphenol by ferrate(VI). J. Hazard. Mater. 401, 123405.

Zimmermann, S.G., Schmukat, A., Schulz, M., Benner, J., Gunten, U., Ternes, T.A., 2012. Kinetic and mechanistic investigations of the oxidation of tramadol by ferrate and ozone. Environ. Sci. Technol. 46, 876–884.